$\mathbf{M}^{\text{odeling}}_{\text{athematical}} \mathbf{C}^{\text{omputing}}$

Influence of the uniaxial stress p_2 and transverse fields E_1 and E_3 on the phase transitions and thermodynamic characteristics of GPI ferroelectric materials

Levitskii R. R.[1], Zachek I. R.[2], Vdovych A. S.[1], Bilenka O. B.[2]

[1] Institute for Condensed Matter Physics, Nat. Acad. of Sci. of Ukraine,
1 Svientsitsky Str., Lviv 79011, Ukraine
[2] Lviv Polytechnic National University,
12 S. Bandera Str., Lviv 79013, Ukraine

A modified GPI model that accounts for the piezoelectric coupling between the ordered structural elements and the strains ε_j has been used for studing of effects arising in GPI ferroelectrics under the action of the uniaxial stress p_2 and electric fields E_1 and E_3. The polarization vectors and components of static dielectric permittivity are calcucated in the two-particle cluster approximation for mechanically clamped crystal, and piezoelectric and thermal parameters are also determined. The influence of the simultaneous action of the stress p_2 and fields E_1 and E_3 on the phase transition and physical characteristics of GPI crystal has been studied.

1. Introduction

The study of the effects these arise under the action of mechanical stresses and external electric fields is one of the actual problems in the physics of ferroactive compounds, in particular, of glycine phosphite crystal (GPI), which belongs to ferroelectric materials with hydrogen bonds [1].

The experimental study of the transverse electric field E_3 on the dielectric permittivity ε_{33} of a GPI crystal was carried out by authors in [2,3]. They showed that the application of the field E_3 leads to decrease of the ferroelectric phase transition temperature.

The model of a deformable GPI crystal were developed in [3], which takes into account a ferroelectric coupling between a proton and lattice subsystems. This model in [6] served as a basis to study the influence of the transverse electric fields E_1 and E_3 on the dielectric and piezoelectric properties of GPI. The above-mentioned experimental data [3] obtained for the temperature dependence of the transverse dielectric permittivity ε_{33} in the presence of the field E_3. It was found that the influence of the field E_1 is qualitatively similar to that of the field E_3, but is an order of magnitude weaker.

In [8] the GPI model [5] was modified to describe the case where the shear stress σ_4, σ_5 and σ_6 are applied to the GPI crystal in the absence of an electric field. It was found that the appearance of the shear stresses σ_4 or σ_6 in the ferroelectric phase gives rise to the emergence of spontaneous polarization along the axes OX and OZ, and the transverse permittivities ε_{11} and ε_{33} tend to infinity at the temperature T_c. And what's more the influence of the stress σ_4 is similar to influence of σ_6. In [7] the influence of mechanical stresses and transverse electric fields on the piezoelectric coefficients of GPI crystal has been studied.

In this work on the basis of the deformed GPI crystal model, the simultaneous action of the uniaxial stress p_2 along ferroelectric axis and transverse electric fields E_1 and E_3 on the phase transition and thermodynamical parameters of these type crystals are investigated.

2. Hamiltonian Model

Let us consider a system of protons in the GPI crystal moving along the O-H...O bonds. These bonds form a zigzag chains along the c-axis of the GPI crystal. Let us assign the dipole moments $\boldsymbol{d}_{qf}(f = 1, \ldots, 4)$ to the proton ($f = 1, \ldots, 4$). In the ferroelectric phase the dipole moments are mutually compensated ($\boldsymbol{d}_{q1}$ with $\boldsymbol{d}_{q3}$, $\boldsymbol{d}_{q2}$ with $\boldsymbol{d}_{q4}$) in the Z-axis and X-directions, and simultaneously mutually added in the Y-direction, thus generating a spontaneous polarization. The vectors $\boldsymbol{d}_{qf}$ are oriented at certain angles with respect to the crystallographic axes and has the longitudinal and transverse components with respect to the b-axis.

Taking into account the short-range and long-range interactions and presence of electric fields E_1, E_2 and E_3 along of positive directions of the Cartesian coordinates X, Y and Z, the Hamiltonian of the GPI proton system equals

$$\hat{H} = NU_{seed} + \hat{H}_{short} + \hat{H}_{long} + \hat{H}_E, \tag{1}$$

where N is the total number of primitive cells in the Bravais lattice. In (1), the quantity U_{seed} is the seed energy correspond to lattice of the hard ions and not depend obviously of the proton subsystem configuration, and consists of elastic, piezoelectric and dielectric parts, which are expressed in terms of the electric fields E_i ($i = 1, 2, 3$) and the strains ε_j ($j = 1, \ldots, 6$) so that.

Other quantities in (1) describe a pseudospin part of the Hamiltonian. In particular a second quantity in (1) is the Hamiltonian of short-range interactions,

$$\hat{H}_{short} = -2\sum_{qq'} \left(w_1 \frac{\sigma_{q1}}{2} \frac{\sigma_{q2}}{2} + w_2 \frac{\sigma_{q3}}{2} \frac{\sigma_{q4}}{2} \right) \left(\delta_{\mathbf{R}_q \mathbf{R}_{q'}} + \delta_{\mathbf{R}_q + \mathbf{R_c}, \mathbf{R}_{q'}} \right). \tag{2}$$

Another quantities in (1) describes a pseudospin part of the Hamiltonian. In particular a second quantity in (1) is the Hamiltonian of short-range interactions. In (2) σ_{qf} is a z-component of the pseudospin operator, which describes the f-th ($f = 1, 2, 3, 4$) bond stage located in the q-th cell. The first and second Kronecker deltas correspond to the proton interaction in the chains located near the HPO$_3$ tetrahedra of types I and II, respectively, and $\mathbf{R_c}$ is the lattice radius vector directed along the c-axis. The values w_1, w_2 describe short-range interactions of protons in the chains. We can expand them into series in the strains ε_j and expansions to the linear terms:

$$w_{1,2} = w^0 + \sum_l \delta_l \varepsilon_l \pm \delta_4 \varepsilon_4 \pm \delta_6 \varepsilon_6, \quad (l = 1, 2, 3, 5) \tag{3}$$

Third addendum in (1), which describes the long-range dipole-dipole and undirect (by means of lattice oscillation) proton-proton interactions, is taken into account with average field approximation:

$$\hat{H}_{long} = NH^0 - \sum_q \sum_{f=1}^{4} \mathcal{H}_f \frac{\sigma_{qf}}{2}, \tag{4}$$

where

$$H^0 = \sum_{f,f'=1}^{4} \frac{1}{8} J_{ff'} \eta_f \eta_{f'}, \quad \mathcal{H}_f = \sum_{f'=1}^{4} \frac{1}{2} J_{ff'} \eta_{f'}, \quad \eta_f = \langle \sigma_{qf} \rangle. \tag{5}$$

Let us lay out the Fourier-modes of the interaction constants $J_{ff'} = \sum_{q'} J_{ff'}(qq')$ at $\mathbf{k} = 0$ in series in the strains ε_j linearly:

$$J_{\underset{33}{11}} = J_{11}^0 + \sum_l \psi_{11l} \varepsilon_l \pm \psi_{114} \varepsilon_4 \pm \psi_{116} \varepsilon_6, \quad J_{13} = J_{13}^0 + \sum_l \psi_{13l} \varepsilon_l + \psi_{134} \varepsilon_4 + \psi_{136} \varepsilon_6,$$

$$J_{\underset{34}{12}} = J_{12}^0 + \sum_l \psi_{12l} \varepsilon_l \pm \psi_{124} \varepsilon_4 \pm \psi_{126} \varepsilon_6, \quad J_{\underset{23}{14}} = J_{14}^0 + \sum_l \psi_{14l} \varepsilon_l \pm \psi_{144} \varepsilon_4 \pm \psi_{146} \varepsilon_6,$$

$$J_{\underset{44}{22}} = J_{22}^0 + \sum_l \psi_{22l} \varepsilon_l \pm \psi_{224} \varepsilon_4 \pm \psi_{226} \varepsilon_6, \quad J_{24} = J_{24}^0 + \sum_l \psi_{24l} \varepsilon_l + \psi_{244} \varepsilon_4 + \psi_{246} \varepsilon_6,$$

The fourth addendum in (1) describes pseudospin interaction with external electric field:

$$\hat{H}_E = -\sum_{qf} \boldsymbol{\mu}_f \boldsymbol{E} \frac{\sigma_{qf}}{2}. \tag{6}$$

Here, $\boldsymbol{\mu}_1 = (\mu_{13}^x, \mu_{13}^y, \mu_{13}^z)$, $\boldsymbol{\mu}_3 = (-\mu_{13}^x, \mu_{13}^y, -\mu_{13}^z)$, $\boldsymbol{\mu}_2 = (-\mu_{24}^x, -\mu_{24}^y, \mu_{24}^z)$, $\boldsymbol{\mu}_4 = (\mu_{24}^x, -\mu_{24}^y, -\mu_{24}^z)$ are effective dipole moments per pseudospin.

When calculating the thermodynamic and dynamic parameters of ferroactive compounds like a GPI type, let us apply the two-particle cluster (TPC) approximation. In this approximation, the thermodynamic potential of GPI per one cell under the action of the shear stresses σ_j has the form

$$g = U_{seed} + H^0 - 2\Big(w^0 + \sum_l \delta_l \varepsilon_l\Big) + 2k_B T \ln 2 - N\upsilon \sum_{i=1}^3 \sigma_i \varepsilon_i - \frac{1}{2} k_B T \sum_{f=1}^4 \ln\big(1 - \eta_f^2\big) - 2k_B T \ln D. \tag{7}$$

According to a thermodynamic potential minimum condition we obtained the system of simultaneous equations for η_f and ε_j. In case of applying the hydrostatic stress to crystal, we obtained: $\sigma_1 = \sigma_2 = \sigma_3 = -p_h \neq 0$, $\sigma_4 = \sigma_5 = \sigma_6 = 0$. Differentiating the balance thermodynamic potential of the fields E_i, we obtained the polarization components P_i:

$$P_1 = e_{14}^0 \varepsilon_4 + e_{16}^0 \varepsilon_6 + \chi_{11}^{\varepsilon 0} E_1 + [\mu_{13}^x(\eta_1 - \eta_3) - \mu_{24}^x(\eta_2 - \eta_4)]/(2v),$$

$$P_2 = e_{21}^0 \varepsilon_1 + e_{22}^0 \varepsilon_2 + e_{23}^0 \varepsilon_3 + e_{25}^0 \varepsilon_5 + \chi_{22}^{\varepsilon 0} E_2 + [\mu_{13}^y(\eta_1 + \eta_3) - \mu_{24}^y(\eta_2 + \eta_4)]/(2v), \tag{8}$$

$$P_3 = e_{34}^0 \varepsilon_4 + e_{66}^0 \varepsilon_6 + \chi_{33}^{\varepsilon 0} E_3 + [\mu_{13}^z(\eta_1 - \eta_3) + \mu_{24}^z(\eta_2 - \eta_4)]/(2v).$$

Static isothermic dielectric permittivities along the axis for mechanically squeezed GPI crystal have the form:

$$\chi_{11}^\varepsilon = \left(\frac{\partial P_1}{\partial E_1}\right)_{\varepsilon_j} = \chi_{11}^{\varepsilon 0} + \frac{1}{2v\Delta}\left[\mu_{13}^x(\Delta_1^{\chi a} - \Delta_3^{\chi x}) - \mu_{24}^x(\Delta_2^{\chi x} - \Delta_4^{\chi x})\right], \tag{9}$$

$$\chi_{22}^\varepsilon = \left(\frac{\partial P_2}{\partial E_2}\right)_{\varepsilon_j} = \chi_{22}^{\varepsilon 0} + \frac{1}{2v\Delta}\left[\mu_{13}^y(\Delta_1^{\chi y} + \Delta_3^{\chi y}) - \mu_{24}^y(\Delta_2^{\chi y} + \Delta_4^{\chi y})\right], \tag{10}$$

$$\chi_{33}^\varepsilon = \left(\frac{\partial P_3}{\partial E_3}\right)_{\varepsilon_j} = \chi_{33}^{\varepsilon 0} + \frac{1}{2v\Delta}\left[\mu_{13}^z(\Delta_1^{\chi z} - \Delta_3^{\chi z}) + \mu_{24}^c(\Delta_2^{\chi z} - \Delta_4^{\chi z})\right]. \tag{11}$$

Here a relation

$$\frac{\Delta_f^{\chi\alpha}}{\Delta} = \left(\frac{\partial \eta_f}{\partial E_\alpha}\right)_{\varepsilon_l}$$

has a sense of local pseudospin permittivity, which describes the f-th order parameter influence on the external electric field E_α at constant deformations.

On the basis of correlations (8), we obtained the expressions for isothermic coefficients of the GPI piezoelectric strain e_{2l}:

$$e_{1j} = \left(\frac{\partial P_1}{\partial \varepsilon_j}\right)_{E_1} = e_{1j}^0 + \frac{\mu_{13}^a}{2v\Delta}(\Delta_{1j}^e - \Delta_{3j}^e) - \frac{\mu_{24}^a}{2v\Delta}(\Delta_{2j}^e - \Delta_{4j}^e), \quad (j = 4, 6), \tag{12}$$

$$e_{2l} = \left(\frac{\partial P_2}{\partial \varepsilon_l}\right)_{E_2} = e_{2l}^0 + \frac{\mu_{13}^b}{2v\Delta}(\Delta_{1l}^e + \Delta_{3l}^e) - \frac{\mu_{24}^b}{2v\Delta}(\Delta_{2l}^e + \Delta_{4l}^e), \quad (l = 1, 2, 3, 5), \tag{13}$$

$$e_{3j} = \left(\frac{\partial P_3}{\partial \varepsilon_j}\right)_{E_3} = e_{3j}^0 + \frac{\mu_{13}^c}{2v\Delta}(\Delta_{1j}^e - \Delta_{3j}^e) + \frac{\mu_{24}^c}{2v\Delta}(\Delta_{2j}^e - \Delta_{4j}^e), \quad (j = 4, 6). \tag{14}$$

Here relations

$$\frac{\Delta_{fl}^e}{\Delta} = \left(\frac{\partial \eta_f}{\partial \varepsilon_l}\right)_{E_2}, \quad \frac{\Delta_{fj}^e}{\Delta} = \left(\frac{\partial \eta_f}{\partial \varepsilon_j}\right)_{E_2}$$

describe the f-th parameter influence on the deformations ε_l, ε_j at constant external fields. Other dielectric, piezoelectric and elastic GPI parameters one can obtain using above calculated correlations.

A modal entropy and thermal capacity conditioned by proton subsystem, we obtained by numerical differentiation of the thermodynamic potential with respect to temperature:

$$S = -N_A \left(\frac{\partial g}{\partial T}\right)_\sigma, \quad \Delta C^\sigma = T \left(\frac{\partial S}{\partial T}\right)_\sigma.$$

3. A comparison of the results of numerical calculations with experimental data

To calculate the temperature dependence of dielectric, elastic, piezoelectric and thermal characteristics of GPI we need to set certain values of the following parameters: parameters of the short-range interactions w^0; parameters of the long-range interactions $\nu_1^{0\pm} = \frac{1}{4}(J_{11}^0 \pm J_{13}^0)$, $\nu_2^{0\pm} = \frac{1}{4}(J_{12}^0 \pm J_{14}^0)$, $\nu_3^{0\pm} = \frac{1}{4}(J_{22}^0 \pm J_{24}^0)$; deformational potentials δ_i, $\psi_{1i}^{\pm} = \frac{1}{4}(\psi_{11i} \pm \psi_{13i})$, $\psi_{2i}^{\pm} = \frac{1}{4}(\psi_{12i} \pm \psi_{14i})$, $\psi_{3i}^{\pm} = \frac{1}{4}(\psi_{22i} \pm \psi_{24i})$ $(i=1,...,6)$; effective dipole moments μ_{13}^x; μ_{24}^x; μ_{13}^y; μ_{24}^y; μ_{13}^z; μ_{24}^z; "seed" dielectric susceptibilities $\chi_{ij}^{\varepsilon 0}$; "seed" coefficients of piezoelectric stress e_{ij}^0; "seed" elastic constants c_{ij}^{E0}.

In order to determine the required values, we used the experimental temperature dependences of the following parameters of GPI: $P_s(T)$ [9], $C_p(T)$ [10], $\varepsilon_{11}^{\sigma}$, $\varepsilon_{33}^{\sigma}$ [1], d_{21}, d_{23} [11], and also the phase transition temperature dependence versus hydrostatic pressure values.

The volume of the GPI unit cell was taken equal to $\upsilon = 0.601 \cdot 10^{-21}$ см^3 [12, 13].

A numerical analysis shows that thermodynamic characteristics depend on two linear combinations for the long-range interactions $\nu^{0+} = \nu_1^{0+} + 2\nu_2^{0+} + \nu_3^{0+}$ and $\nu^{0-} = \nu_1^{0-} + 2\nu_2^{0-} + \nu_3^{0-}$ and do not depend (deviation <0.1%) on six concrete values $\nu_f^{0\pm}$ at given values ν^{0+} and ν^{0-}. Optimal values for these combinations are obtained $\nu^{0+}/k_B = 12.26\,\text{K}$, $\nu^{0-}/k_B = 0.2\,\text{K}$; for concrete $\nu_f^{0\pm}$ we choose $\tilde{\nu}_1^{0+} = \tilde{\nu}_2^{0+} = \tilde{\nu}_3^{0+} = 3.065\,\text{K}$, $\tilde{\nu}_1^{0-} = \tilde{\nu}_2^{0-} = \tilde{\nu}_3^{0-} = 0.05\,\text{K}$, where $\tilde{\nu}_f^{0\pm} = \nu_f^{0\pm}/k_B$.

For $\psi_{fi}^{\pm}$-parameters, by analogy to with $\nu_f^{0\pm}$-parameters, six linear combinations for $\psi_i^{+} = \psi_{1i}^{+} + 2\psi_{2i}^{+} + \psi_{3i}^{+}$ and six combinations $\psi_i^{-} = \psi_{1i}^{-} + 2\psi_{2i}^{-} + \psi_{3i}^{-}$ are very important. The thermodynamic parameters do not depend practically (deviation $< 0.1\%$) for the 36 concrete values of $\psi_{fi}^{\pm}$ at given values for ψ_i^{+} and ψ_i^{-}.

The optimal values for $\psi_{fi}^{\pm}$ are follows: $\tilde{\psi}_{f1}^{+} = 93.6\,\text{K}$, $\tilde{\psi}_{f2}^{+} = 252.5\,\text{K}$, $\tilde{\psi}_{f3}^{+} = 110.7\,\text{K}$, $\tilde{\psi}_{f4}^{+} = \tilde{\psi}_{f6}^{+} = \tilde{\psi}_{f4}^{-} = \tilde{\psi}_{f6}^{-} = 79.5\,\text{K}$, $\tilde{\psi}_{f5}^{+} = 22.7\,\text{K}$, $\tilde{\psi}_{f1}^{-} = \tilde{\psi}_{f2}^{-} = \tilde{\psi}_{f3}^{-} = \tilde{\psi}_{f5}^{-} = 0\,\text{K}$, where $\tilde{\psi}_{fi}^{\pm} = \psi_{fi}^{\pm}/k_B$.

The parameter of the short-range interaction $w_0(x)/k_B = 800\,\text{K}$.

The optimal values found for the deformation potentials δ_j, which are distribution coefficients of parameter w_0 in deformations ε_j: $\tilde{\delta}_1 = 500\,\text{K}$, $\tilde{\delta}_2 = 600\,\text{K}$, $\tilde{\delta}_3 = 500\,\text{K}$, $\tilde{\delta}_4 = 150\,\text{K}$, $\tilde{\delta}_5 = 100\,\text{K}$, $\tilde{\delta}_6 = 150\,\text{K}$, $\tilde{\delta}_i = \delta_i/k_B$.

The effective dipole moments in the paraphase are $\mu_{13}^x = 0.4 \cdot 10^{-18}$esu·cm; $\mu_{13}^y = 4.05 \cdot 10^{-18}$esu·cm; $\mu_{13}^z = 4.2 \cdot 10^{-18}$esu·cm; $\mu_{24}^x = 2.3 \cdot 10^{-18}$esu·cm; $\mu_{24}^y = 3.0 \cdot 10^{-18}$esu·cm; $\mu_{24}^z = 2.2 \cdot 10^{-18}$esu·cm.

In the ferrophase, the y-component of the first dipole moment equals $\mu_{13ferro}^y = 3.82 \cdot 10^{-18}$esu·cm.

The values of the "seed" piezoelectric coefficients susceptibilites and elastic constants: $e_{ij}^0 = 0.0\,\frac{\text{esu}}{\text{cm}^2}$; $\chi_{11}^{\varepsilon 0} = 0.1$, $\chi_{22}^{\varepsilon 0} = 0.403$, $\chi_{33}^{\varepsilon 0} = 0.5$, $\chi_{13}^{\varepsilon 0} = 0.0$; $c_{11}^{0E} = 26.91 \cdot 10^{10}\,\frac{\text{dyn}}{\text{cm}^2}$, $c_{12}^{E0} = 14.5 \cdot 10^{10}\,\frac{\text{dyn}}{\text{cm}^2}$, $c_{13}^{E0} = 11.64 \cdot 10^{10}\,\frac{\text{dyn}}{\text{cm}^2}$, $c_{15}^{E0} = 3.91 \cdot 10^{10}\,\frac{\text{dyn}}{\text{cm}^2}$, $c_{22}^{E0} = (64.99 - 0.04(T - T_c)) \cdot 10^{10}\,\frac{\text{dyn}}{\text{cm}^2}$, $c_{23}^{E0} = 20.38 \cdot 10^{10}\,\frac{\text{dyn}}{\text{cm}^2}$, $c_{25}^{E0} = 5.64 \cdot 10^{10}\,\frac{\text{dyn}}{\text{cm}^2}$, $c_{33}^{E0} = 24.41 \cdot 10^{10}\,\frac{\text{dyn}}{\text{cm}^2}$, $c_{35}^{E0} = -2.84 \cdot 10^{10}\,\frac{\text{dyn}}{\text{cm}^2}$, $c_{55}^{E0} = 8.54 \cdot 10^{10}\,\frac{\text{dyn}}{\text{cm}^2}$, $c_{44}^{E0} = 15.31 \cdot 10^{10}\,\frac{\text{dyn}}{\text{cm}^2}$, $c_{46}^{E0} = -1.1 \cdot 10^{10}\,\frac{\text{dyn}}{\text{cm}^2}$, $c_{66}^{E0} = 11.88 \cdot 10^{10}\,\frac{\text{dyn}}{\text{cm}^2}$.

The dependencens of the phase transition temperature T_c on electric fields E_1 and E_3 and pressure p_2 are presented in Fig. 1 and 2 respectively. If the fields E_1 and E_3 are increase then the phase transition temperature T_c decrease, especially for E_3.
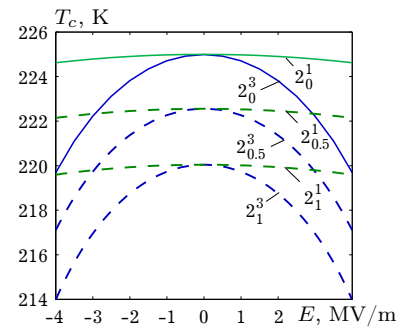

Fig. 1. Temperature T_c dependence on electric fields E_1 (curves 1) and $E_3(3)$ (3) at different values of uniaxial pressure p_2 (GPa). Superscript corresponds to the magnitude of the field, and subscript corresponds to the pressure values.
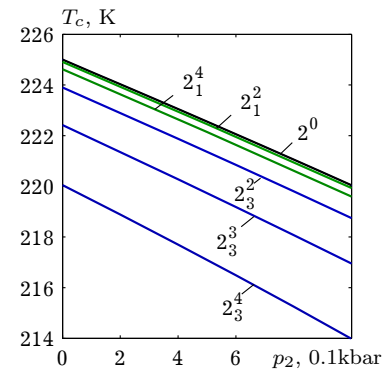

Fig. 2. Dependence of temperature T_c on uniaxial pressure p_2 at different values of electric fields E_1 and E_3. Superscript corresponds to the direction of field, and subscript corresponds to the magnitudes of the fields $E_1(1)$ and $E_3(3)$ (MV/m).

The temperature dependences of the GPI crystal polarization P_i at various values of the electric field strength E_1 are shown in Fig. 3, the same at various values of the electric field strength E_3 are shown in Fig. 4.
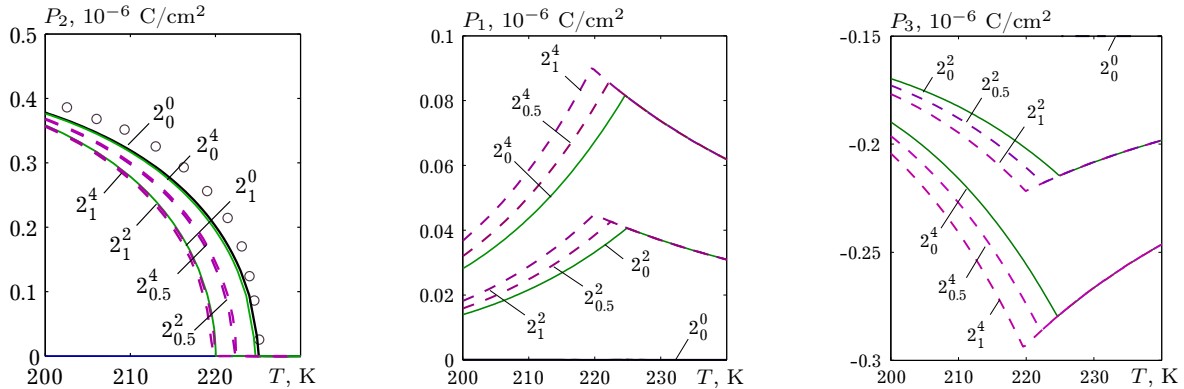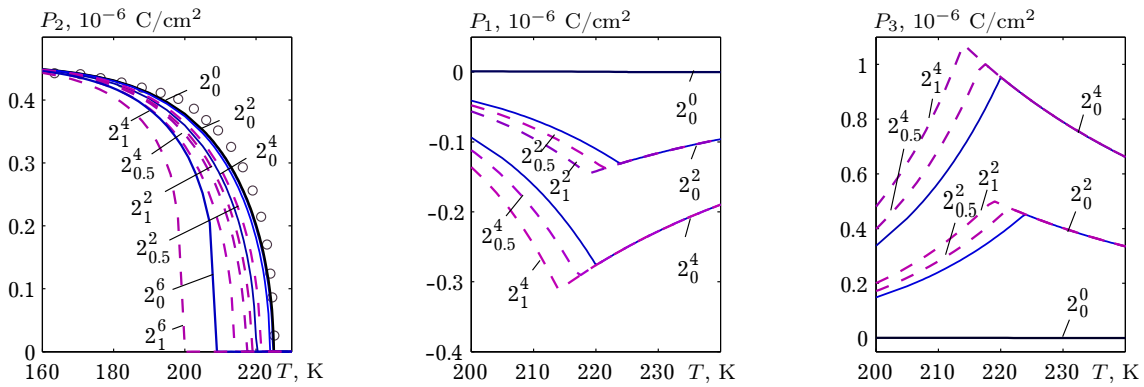

Fig. 3. The temperature dependences of the components of polarization P_2, P_1, P_3 of GPI crystal at different values of uniaxial pressure p_2 (GPa) and at different values of electric field E_1 (MV/m). Superscript corresponds to the magnitude of the field, and subscript corresponds to the pressure values. ∘ are the experimental data [9].

Fig. 4. The temperature dependences of the components of polarization P_2, P_1, P_3 of GPI crystal at different values of uniaxial pressure p_2 (GPa) and at different values of electric fields E_3 (MV/m). Superscript corresponds to the magnitude of the field, and subscript corresponds to the pressure values. ∘ are the experimental data [9].

According to the increase of strength E_1, the spontaneous polarization P_2 is insignificantly decreasing and induced by field polarization P_1 is increasing. Polarization P_3 induced by field E_1 is a negative and three times greater than P_1.

Temperature dependence of negative polarization $P_3(E_1)$ induced by field E_3 is analogous to $P_3(E_1)$, and $P_1(E_3)$ value almost egual to $P_3(E_1)$.
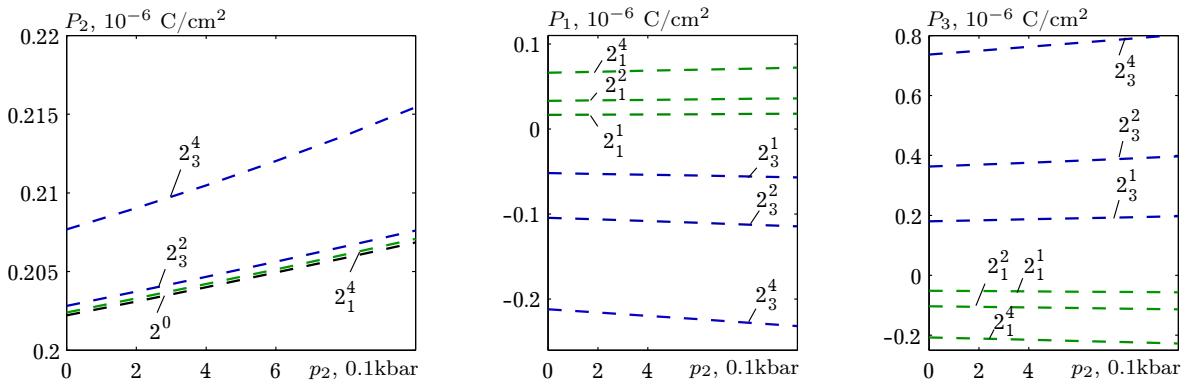

Fig. 5. The dependence of polarization P_i of GPI crystal on uniaxial pressure p_2 at different values of electric fields E_1 and E_3. The superscript corresponds to the magnitude of the field, and subscript corresponds to the magnitudes of the fields $E_1(1)$ and $E_3(3)$ at the temperature $\Delta T = -5\,\mathrm{K}$.

If the pressure p_2 is applied and that not lead to induction of the polarization P_1 and P_3, then simultaneous effect of pressure and fields (p_2, E_1), (p_2, E_3) intensify the result of influence to fields P_1 and P_3 separately.

When identical deflection from transition temperature T_c (in particular $\Delta T = -5\,\mathrm{K}$) the polarization components P_1, P_2, P_3 of the GPI crystal at various values of electric fields E_1 and E_3 practically linearly depends on pressure p_2 (Fig. 5). Only polarization P_2 shows the increase at pressure increase, and values of induced P_1, P_3 are not changed practically.

The polarization components P_1, P_2, P_3 of GPI crystal practically linear depend on transverse electric fields E_1 and E_3 at different values of pressure $_2$ and temperature T . (Fig. 6).

The temperature dependence of the components of dielectric permittivity $\varepsilon_{ii} = 1 + 4\pi\chi_{ii}$ of mechanically clamped GPI crystal under influence of the transverse electric fields E_1 and E_3 are shown in Figs. 7–9.

Separated application of pressure $_2$ to GPI crystal leads to shift of maximum on the temperature dependences of permittivity ε_{22} to lower temperatures (Fig. 7). And applying of fields E_1 and E_3 or simultaneous effect of pressure and fields (p_2, E_1), (p_2, E_3) leads to the finite values of permittivity ε_{22}.

The trasverse permittivities $\varepsilon_{11}(E_1)$, $\varepsilon_{33}(E_1)$ increase slightly in ferroelectric phase,
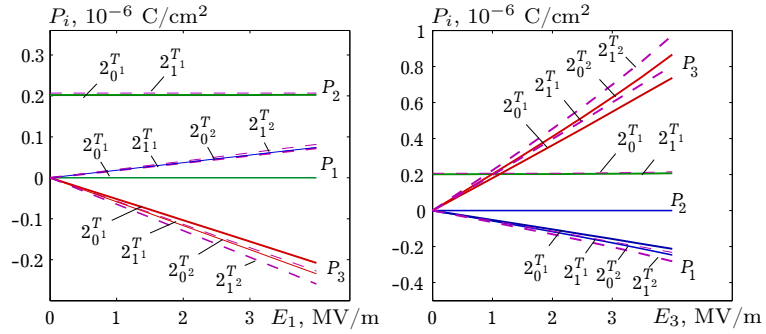

Fig. 6. The dependence of polarization P_i of GPI crystal on electric fields E_1 and E_3 at different values of uniaxial pressure p_2. Superscript corresponds to the temperatures $T_1 = 220\,\mathrm{K}$ and $T_2 = 230\,\mathrm{K}$, and subscript corresponds to the pressure (GPa).
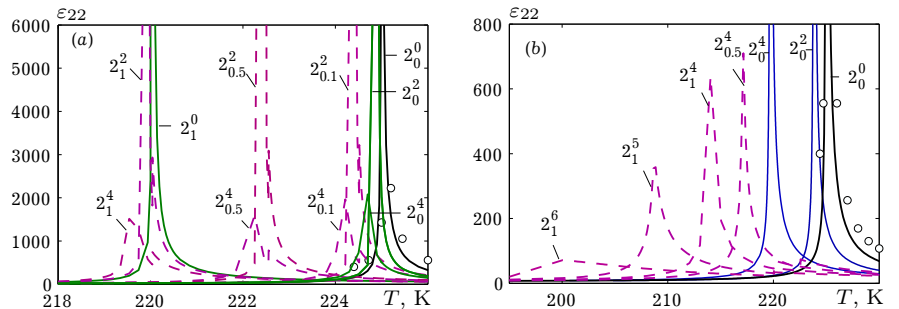

Fig. 7. The temperature dependences of static permeability ε_{22} of GPI crystal at different uniaxial pressure values p_2 (GPa) and at different values of electric field E_1 (a) and E_3 (b) (MV/m). Superscript corresponds to the field magnitude, and subscript corresponds to the pressure. $\circ$ — [14].
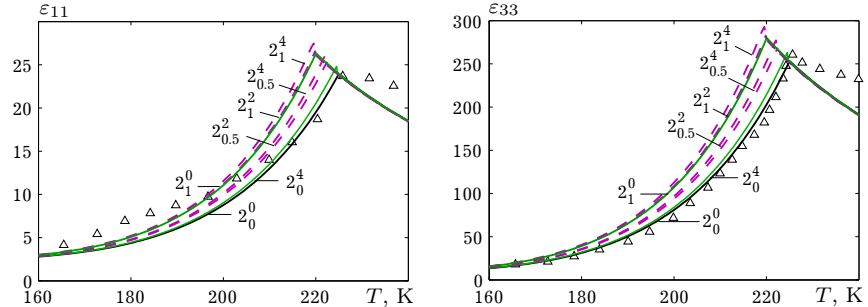

Fig. 8. The temperature dependences of dielectric permittivities of GPI crystal ε_{11} and ε_{33} at different uniaxial pressure values p_2 (GPa) and at different values of electric field E_1 (MV/m). Superscript corresponds to the field magnitude, and subscript corresponds to the pressure. $\triangle$ — [1].
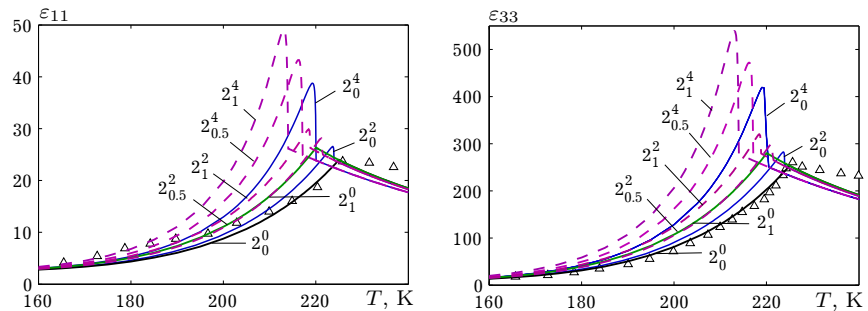

Fig. 9. The temperature dependences of dielectric permittivities of GPI crystal ε_{11} and ε_{33} at different uniaxial pressure values p_2 (GPa) and at different values of electric field E_3 (MV/m). Superscript corresponds to the field magnitude, and subscript corresponds to the pressure. $\triangle$ — [1].

and gently decrease in paraphase. Influence of field E_3 displays significantly. In temperature course of permittivities $\varepsilon_{11}(E_3)$ and $\varepsilon_{33}(E_3)$ at phase transition temperatures the sharp maximum in ferroelectric phase near temperature T_c are observed, which are increase when field E_3 increases and shift to lower temperatures side.
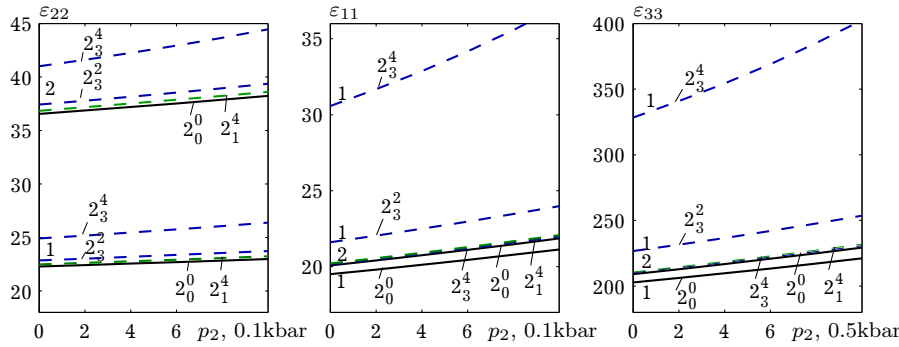

Fig. 10. The dependences of dielectric permittivities ε_{ii} of GPI crystal on uniaxial pressure p_2 at different fields E_1 and E_3 magnitudes. Superscript corresponds to the field magnitude, and subscript corresponds to the fields $E_1(1)$ or $E_3(3)$ at different values of temperature ΔT, K: -5, 1; 10, 2.
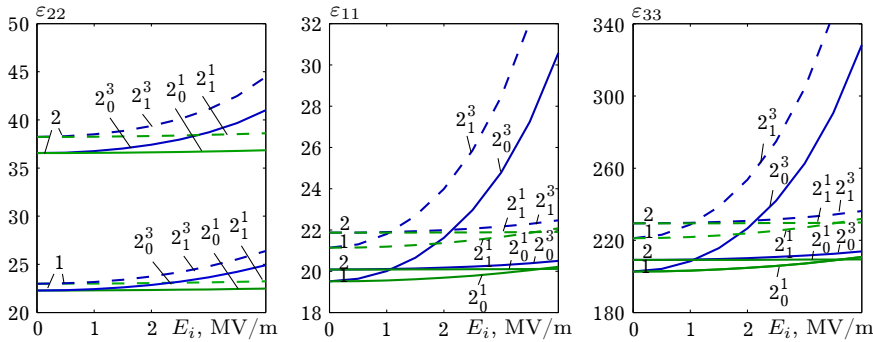
A simultaneous effect of pressure and fields (p_2, E_1), (p_2, E_3) leads to increase of permittivities $\varepsilon_{11}(E_3)$ and $\varepsilon_{33}(E_3)$ at ferroelectric phase (Figs. 10, 11).

The temperature dependences of longitudinal piezoelectric coefficients e_{21} and h_{21} of GPI crystal at different values of electric field E_1 and pressure p_2 are shown in Fig. 12, and at different values of electric field E_3 and pressure p_2 are shown in Fig. 13. When field and pressure values increase, piezoelectric coefficients curves e_{21} and h_{21} shift to less temperature side, and coefficients e_{21} are definite at $T = T_c$, and what is more at field E_3 the maximum of e_{21} significantly smaller than at field E_1.

Fig. 11. The dependences of dielectric permittivities ε_{ii} of GPI crystal on electric fields E_1 and E_3 at different uniaxial pressure p_2 values for the different temperatures ΔT, K: -5, 1; 10, 2. Superscript corresponds to the pressere magnitude, and supebscript corresponds to the fields E_1 (1) or E_3 (3).
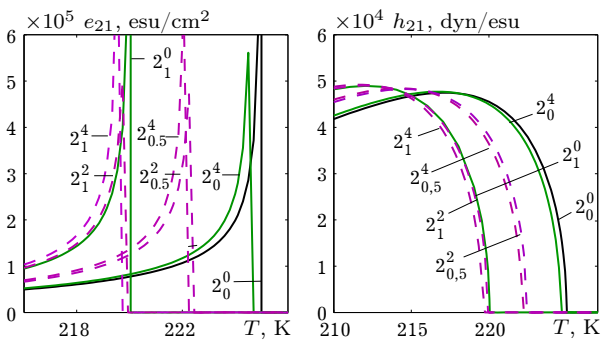

Fig. 12. The temperature dependences of piezoelectric coefficients e_{21} and h_{21} of GPI crystal at different uniaxial pressure p_2 (GPa) and at different values of electric field E_1 (MV/m). Superscript corresponds to the field magnitude, and subscript corresponds to the pressure.
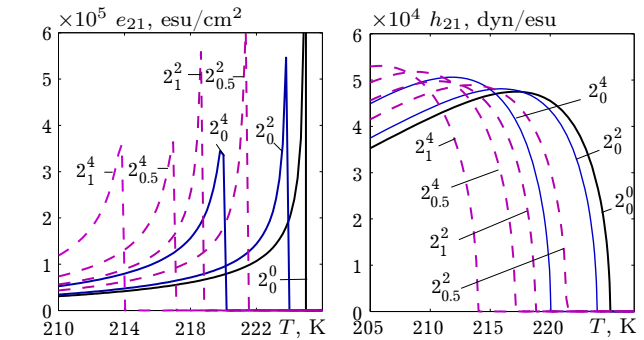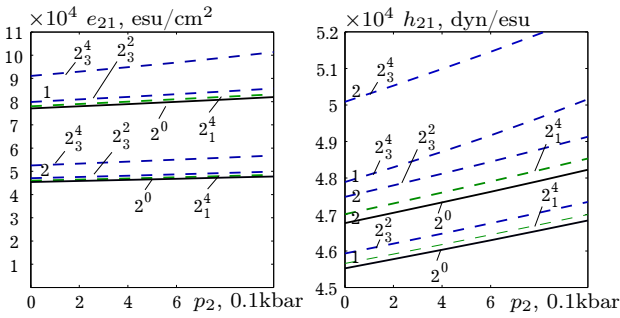
Fig. 13. The temperature dependences of piezoelectric coefficients e_{21} and h_{21} of GPI crystal at different uniaxial pressure p_2 (GPa) and at different values of electric field E_3 (MV/m). Superscript corresponds to the field magnitude, and subscript corresponds to the pressure.

When uniaxial pressure p_2 increases, values of piezoelectric coefficients e_{21} and h_{21} at different electric fields h_{21} and E_3 linearly increase (Fig. 14).

Temperature dependences of the trasverse coefficients e_{14}, e_{34} and h_{14}, h_{34} at different values of electric field E_1 and pressure p_2 are shown in Figs. 16 and 17, and of field E_3 and pressure p_2 are shown in Figs. 15 and 18.

Fig. 14. The dependences of piezoelectric coefficients e_{21} and h_{21} of GPI crystal on uniaxial pressure p_2 for different magnitudes of electric fields E_1 and E_3. Superscript corresponds to the field magnitude, and subscript corresponds to the fields E_1 (1) or E_3 (3) at the different temperatures ΔT, K: -5 - 1; 10-2.
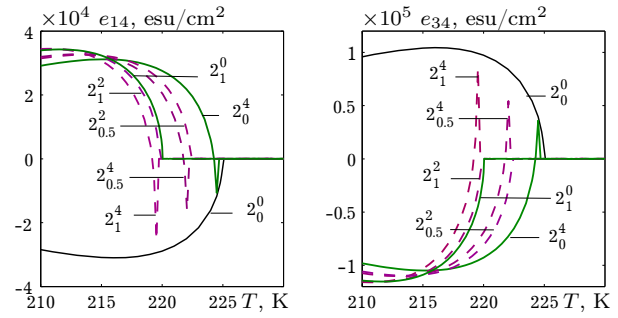

Fig. 15. The temperature dependences of piezoelectric coefficients e_{14} and e_{34} of GPI crystal for different uniaxial pressure values p_2 (GPa) and for different electric field E_3 (MV/m) values. Superscript corresponds to the field magnitude, and subscript corresponds to the magnitudes of pressure.
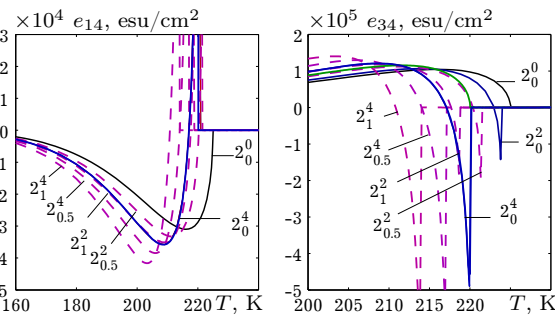

Fig. 16. The temperature dependences of piezoelectric coefficients e_{14} and e_{34} of GPI crystal for different uniaxial pressure values p_2 (GPa) and for different electric field E_1 (MV/m) values. Superscript corresponds to the field magnitude, and subscript corresponds to the pressure.

Fig. 17. The temperature dependences of piezoelectric coefficients h_{14} and h_{34} of GPI crystal for different uniaxial pressure values p_2 (GPa) and for different electric field E_1 (MV/m) values. Superscript corresponds to the field magnitude, and subscript corresponds to the pressure.
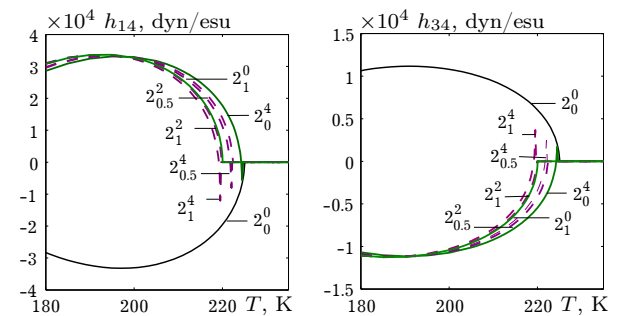
The piezoelectric coefficients e_{14}, h_{14}, at temperature close to T_c, are describes by finite peak-like curves, their maximums increase with increasing of field E_3, but coefficients e_{34}, and h_{34} decrease with increasing of field up to appearance of negative depression near T_c. This depression has finite value.

Influence of field E_1 on piezoelectric coefficients looks like influence of field E_3, but an order of magnitude weaker.

When the pressure p_2 applied to the crystal is increased along the ferroelectric axis, coefficient e_{14} value decreases slightly linearly, and e_{34} increases in this way (Fig. 19). Coefficients h_{14} and h_{34} with pressure change are practically unchanged (Fig. 20).

If there is still an electric field E_3, the coefficient e_{14} also decreases slightly linearly, coefficient e_{34} increases with pressure p_2, when applied the field E_1 of the coefficient e_{14} is slightly linearly increased, the coefficient e_{34} decreases.
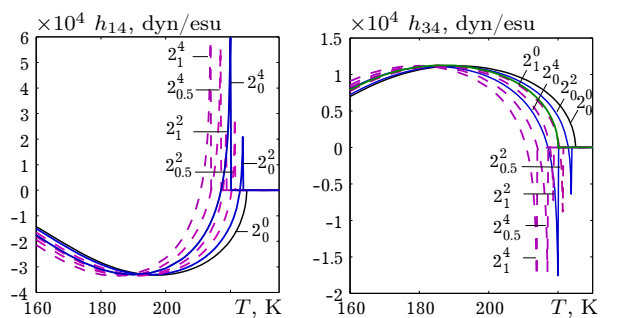

Fig. 18. The temperature dependences of piezoelectric coefficients h_{14} and h_{34} of GPI crystal for different uniaxial pressure values p_2 (GPa) and for different electric field E_3 (MV/m) values. Superscript corresponds to the field magnitude, and subscript corresponds to the pressure.

The temperature dependence of the proton contribution into molar heat capacity does not change qualitatively under uniaxial pressure p_2 and transverse field components E_1 and E_3 (Fig. 21). With increasing of pressure p_2 and fields E_1 and E_3 the ΔC_p value is slightly reduced and this effect is reduced by an increase in temperature ΔT (Fig. 21).
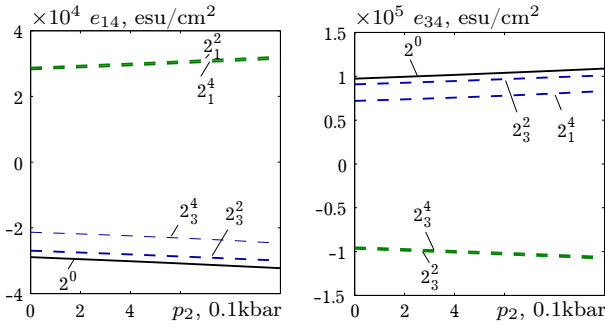
Fig. 19. The dependences of piezoelectric coefficients e_{14} and e_{34} of GPI crystal on uniaxial pressure p_2 for different electric fields E_1 and E_3 values. Superscript corresponds to the field magnitude, and subscript corresponds to the fields E_1 (1) or E_3 (3) at the temperature $\Delta T = -5\,\mathrm{K}$.

Fig. 20. The dependences of piezoelectric coefficients h_{14} and h_{34} of GPI crystal at uniaxial pressure p_2 for different electric fields E_1 and E_3 values. Superscript corresponds to the field magnitude, and subscript corresponds to the fields E_1 (1) or E_3 (3) on the temperature $\Delta T = -5\,\mathrm{K}$.
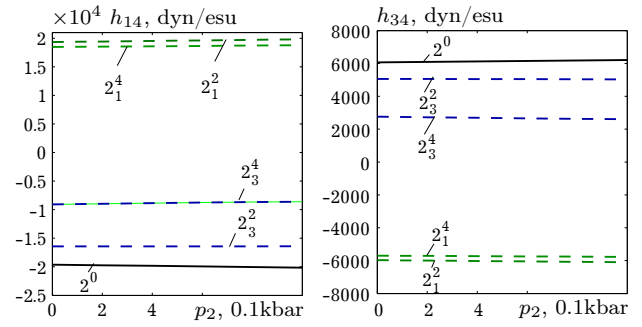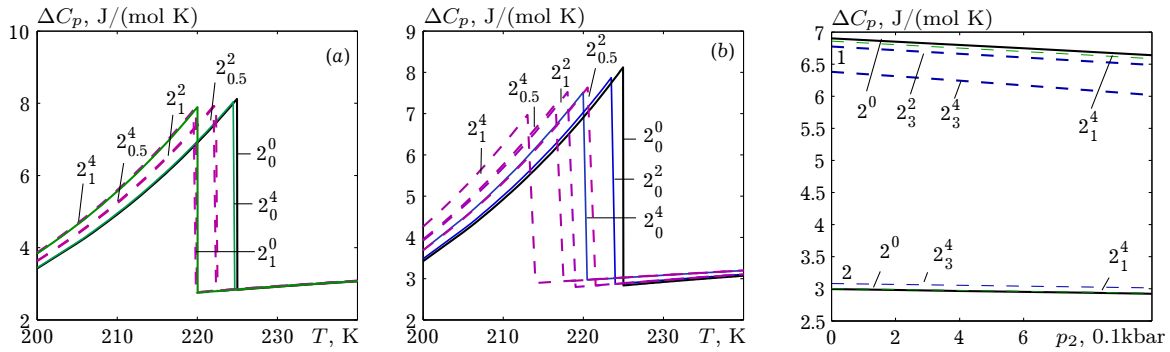

Fig. 21. The temperature dependence of proton contribution to the molar heat capacity ΔC_p of GPI crystal at different values of uniaxial pressure p_2 (GPa) and at different values of electric field $E_1(a)$ (a) and $E_3(b)$ (MV/m) (b) (MV/m). Superscript corresponds to the field magnitude, and subscript corresponds to the pressure and dependence ΔC_p at uniaxial pressure p_2 for different electric fields E_1 and E_3. Superscript corresponds to the field magnitude, and subscript corresponds to the field E_1 (1) or E_3 (3) at different values of ΔT, K: -5 , 1; 10, 2.

4. Conclusions

In this work within the modified proton ordering model of quasione-dimension GPI type ferroelectrics with hydrogen bonds taking into account of piezoelectric couping with strains ε_j in the two-particle cluster approximation the influence of the combined effects of the uniaxial pressure p_2 and electric fields E_1 and E_3 on the phase transition and physical characteristics of the GPI ferroelectric was studied.

Applying only the transverse field E_1 or E_3 in the absence of mechanical stresses in the ferroelectric phase slightly increases the ordering of pseudo-spines in chain "A", and significantly reduces ordering in the chain "B". As a result, the temperature T_c decreases, the trasverse components of permitivities ε_{11} and ε_{33} increase significantly and polarization components P_1 and P_3 are induced in the whole temperature range.

Thermodynamic characteristics under pressure p_2 and fields E_1 and E_3 crystal are shifted the lower temperatures.

In the presence of fields, the coefficients e_{21} are finite at the transition temperature $T = T_c$.

Piezoelectric coefficients e_{14}, h_{14} in the presence of the fields E_3 and E_1 and pressure p_2 are also finite at the temperatures close to T_c.

To perform numerical calculations of thermodynamic characteristics with regard to pressure p_2 and fields E_1 and E_3 we do not use additional parameters compared to calculations without external fields. Therefore, the resulting temperature dependences of the thermodynamic characteristics of GPI crystal have the character of prediction.

[1] Dacko S., Czapla Z., Baran J., Drozd M. Ferroelectricity in Gly·H$_3$PO$_3$ crystal. Physics Letters A. **223** (3), 217–220 (1996).

[2] Stasyuk I., Czapla Z., Dacko S., Velychko O. Proton ordering model of phase transitions in hydrogen bonded ferrielectric type systems: the GPI crystal. Condens. Matter Phys. **6** (3), 483–498 (2003).

[3] Stasyuk I., Czapla Z., Dacko S., Velychko O. Dielectric anomalies and phase transition in glycinium phosphite crystal under the influence of a transverse electric field. J. Phys.: Condens. Matter. **16** (12), 1963–1979, (2004).

[4] Stasyuk I., Velychko O. Theory of Electric Field Influence on Phase Transition in Glycine Phosphite. Ferroelectrics. **300** (1), 121–124 (2004).

[5] Zachek I. R., Shchur Ya., Levitskii R. R., Vdovych A. S. Thermodynamic properties of ferroelectric NH$_3$CH$_2$COOH·H$_2$PO$_3$ crystal. Physica B. **520**, 164–173 (2017).

[6] Zachek I. R., Levitskii R. R., Vdovych A. S., Stasyuk I. V. Influence of electric fields on dielectric properties of GPI ferroelectric. Condens. Matter Phys. **20** (2), 23706 (2017).

[7] Vdovych A., Zachek I., Levitskii R. Calculation of transverse piezoelectric characteristics of quasi-one-dimensional glycine phosphite ferroelectric. Mathematical Modeling and Computing. **5** (2), 242–252 (2018).

[8] Zachek I. R., Levitskii R. R., Vdovych A. S. Deformation effects in glycinium phosphite ferroelectric. Condens. Matter Phys. **21** (3), 33702 (2018).

[9] Nayeem J., Kikuta T., Nakatani N., Matsui F., Takeda S.-N., Hattori K., Daimon H. Ferroelectric Phase Transition Character of Glycine Phosphite. Ferroelectrics. **332** (1), 13–19 (2006).

[10] Shikanai F., Hatori J., Komukae M., Czapla Z., Osaka T. Heat Capacity and Thermal Expansion of NH$_3$CH$_2$COOH·H$_2$PO$_3$. J. Phys. Soc. Jpn. **73** (7), 1812–1815 (2004).

[11] Wiesner M. Piezoelectric properties of GPI crystals. Phys. Stat. Sol (b). **238** (1), 68–74 (2003).

[12] Yasuda N., Sakurai T., Czapla Z. Effects of hydrostatic pressure on the paraelectric–ferroelectric phase transition in glycine phosphite (Gly·H$_3$PO$_3$). J. Phys.: Condens Matter. **9** (23), L347–L350 (1997).

[13] Yasuda N., Kaneda A., Czapla Z. Effects of hydrostatic pressure on the paraelectric–ferroelectric phase transition in deuterated glycinium phosphite crystals. J. Phys.: Condens Matter. **9** (33), L447–L450 (1997).

[14] Nayeem J., Wakabayashi H., Kikuta T., Yamazaki T., Nakatani N. Ferroelectric Properties of Deuterated Glycine Phosphite. Ferroelectrics. **269**, 153–158 (2002).

Вплив одновісного тиску p_2 та поперечних полів E_1 і E_3 на фазові переходи та термодинамічні характеристики сегнетоактивних матеріалів GPI

Левицький Р. Р.[1], Зачек І. Р.[2], Вдович А. С.[1], Біленька О. Б.[2]

[1]*Інститут фізики конденсованих систем НАН України,*
вул. Свєнціцького, 1, Львів, 79011, Україна
[2]*Національний університет "Львівська політехніка",*
вул. С. Бандери 12, 79013, Львів, Україна

Для дослідження ефектів, що виникають під дією одновісного тиску p_2 і електричних полів E_1 та E_3, використано модифіковану модель GPI шляхом врахування п'єзоелектричного зв'язку структурних елементів, які впорядковуються, з деформаціями ε_j. В наближенні двочастинкового кластера розраховано вектори поляризації та компоненти тензора статичної діелектричної проникності механічно затиснутого кристала, їх п'єзоелектричні та теплові характеристики. Досліджено одночасну дію тиску p_2 і полів E_1 та E_3 на фазовий перехід та фізичні характеристики кристала.

Ключові слова: *сегнетоелектрики, фазовий перехід, діелектрична проникність, п'єзомодулі, зсувна напруга.*